AN SGBEM IMPLEMENTATION OF CRACK PROPAGATION AT A FIBRE-MATRIX INTERFACE

J. Kšiňan*, R. Vodička

Technical University of Košice, Civil Engineering Faculty, Vysokoškolská 4, 042 00, Košice, Slovakia
* *Corresponding Author: jozef.ksinan@tuke.sk*

Keywords: interface crack growth, fibre-matrix interface, SGBEM model, debonding process, cohesive type contact, frictional contact, viscous regularization,

Abstract

A new numerical failure model of a cohesive fibre-matrix interface is presented. The contribution discusses the failure mechanism of a fibre bundle embedded in an elastic matrix subjected to transverse tension load. The numerical analysis investigates two subsequent fracture effects: the crack onset and the crack propagation in the fibre-matrix interface. The concept of the solution process presents an SGBEM formulation which includes cohesive-contact interface. The developed mathematical model provides a suitable elucidation of the crack onset and growth in accordance with experimental observations and enables its applicability in the area of composite materials.

1. Introduction

The number of applications of the inter-fibre failure mechanism is increasing in recent years, mostly the applications in the area of the composite materials used in aircraft industry. Therefore, the numerical analysis of contact problems at fibre-matrix interface with effects of friction and viscosity may be very challenging. There exist several approaches for the solution of contact problems by Boundary Element Method, see e.g. [7] and references therein. The present study tries to enhance the energetic model of the fibre-matrix debonding proposed in [2] in order to cover also the frictional contact between the debonded parts of the inclusion. The paper documents the influence of the transversal tension load on the onset and growth of the debonds in the fibre bundle during the whole loading process. In the present work, the frictional law is regularized to cope with the energetic character of the model, see [6]. The regularization is proposed so that convex quadratic energy functionals are obtained and algorithms of quadratic programming can successfully be applied. This includes, first, replacing of the standard Signorini contact conditions by normal compliance contact condition replacement, which allows a small overlapping of solids in contact, and, second, making the bulk domains visco-elastic. In the following sections the proposed model is described in detail, its numerical solution is outlined and a presented example documents the applicability of proposed approach in the area of composite materials.

2. The interface contact model

For the sake of simplicity, only two-dimensional contact problems between two solids, Ω^η ($\eta = A, B$), will be considered in the description of the model. The standard *Signorini condition of unilateral contact* $t_n[\mathbf{u}]_n=0$, $t_n\leq 0$, $[\mathbf{u}]_n\geq 0$ in the contact zone Γ_c is replaced by the normal compliance penalization condition $t_n=k_g[\mathbf{u}]_n^-$, where $[\mathbf{u}]_n^-$ denotes the negative part of the relative normal displacement. This penalization can also be explained by presence of a very thin layer of the normal stiffness $k_g \gg 0$ which is compressed in contact and stress-free out of contact. Here, the relative normal displacement $[\mathbf{u}]_n=(\mathbf{u}^B-\mathbf{u}^A)\cdot\mathbf{n}^A$ is defined at the contact zone. Similarly, the relative tangential displacement $[\mathbf{u}]_s$ can be also defined at the interface, as shown in Figure 1. Also, $\mathbf{t}$ denotes the traction vector and t_n its normal component.

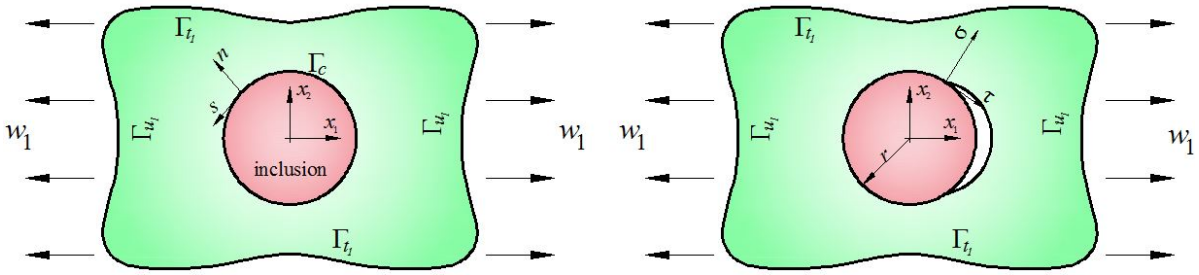

Figure 1. An fibre-matrix interface contact - fibre inclusion problem configuration subjected to transversal loading (a) without and (b) with a partial debond according to [5].

The solution of the contact problem is based on the evolution of energies during the loading process: the elastic energy stored in the bulks and the energy dissipated due to friction and due to viscosity. From a physical point of view, frictional dissipation in our model is given by the functional $\mathcal{R}(\mathbf{u};\dot{\mathbf{u}})=\int_{\Gamma_c} -\mu k_g[\mathbf{u}]_n^-\cdot[\dot{\mathbf{u}}]_s \mathrm{d}\Gamma$, where the rate of the relative tangential displacement $[\mathbf{u}]_s$ is denoted $[\dot{\mathbf{u}}]_s$. The model also includes the classical *Coulomb friction law* $|t_s|\leq\mu|t_n|$ with a constant friction coefficient $\mu\geq 0$ as a relation between normal and tangential tractions, t_n and t_s. The viscosity is considered by a simple linear *Kelvin-Voigt* model which provides the stress tensor σ by the relation $\sigma=\mathbf{C}:\varepsilon(\mathbf{u})+\mathbf{D}:\varepsilon(\dot{\mathbf{u}})$ where $\mathbf{D}$ expresses the fourth-order tensor of viscosity parameters, given in the present work as $\mathbf{D}=\tau_R\mathbf{C}$, where $\tau_R\geq 0$ is a time relaxation parameter.

2.1. Cohesive-type contact

Actual trends at engineering practise usually consider an approach which supposes the non-linear continuous material response of the mechanical stress σ and damage parameter ζ. This approach thus refers to a *cohesive-type model*. An effective approach to achieve the continuous non-linear material response is by means of the energy approach formulation of the *stored energy functional* $\mathcal{E}$, see [3]. The failure mechanism starts, when the mechanical stress σ, linearly increasing with u until the *driving force* σ_d is achieved, reaches activations threshold *fracture energy* G_d . Consequently, ζ starts to evolve from one non-linearly until it arrives to zero, see Figure 2. This can be obtained by adding a new delamination quadratic term ζ^2 and a stiffness parameter k_2 so that the mechanical stress decays as

$$\sigma = \left(k_1\zeta + k_2\zeta^2\right)u. \tag{1}$$

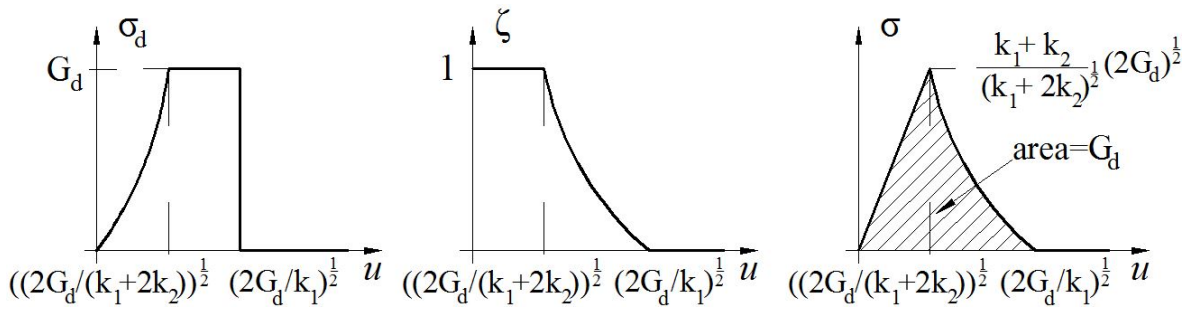

Figure 2. Cohesive contact response of the driving force σ_d, the damage ζ and the mechanical stress σ.

The main feature of the proposed cohesive model is that energy functional is separately quadratic both in the $\mathbf{u}$ and ζ variable. Therefore, it enables to apply *quadratic programming algorithms* for solving *minimization problem*, see [1], [6]. Based on the above assumptions, a quasi-static visco-elastic evolution is governed by the following inclusions:

$$\begin{aligned} \partial_{\mathbf{u}}\mathcal{E}(\tau,\mathbf{u},\zeta) + \mathcal{R}_{\dot{\mathbf{u}}}(\mathbf{u};\dot{\mathbf{u}},\dot{\zeta}) + \delta_{\mathbf{u}}\mathcal{F}(\tau,\mathbf{u}) &\ni 0, \\ \partial_{\zeta}\mathcal{E}(\tau,\mathbf{u},\zeta) + \mathcal{R}_{\dot{\zeta}}(\mathbf{u};\dot{\mathbf{u}},\dot{\zeta}) &\ni 0, \end{aligned} \tag{2}$$

where the symbol ∂ refers to partial subdifferential relying on the convexity of the energy functionals, see [2], [3]. It includes the stored energy functional [3], in a form:

$$\begin{aligned} \mathcal{E}(\tau,\mathbf{u},\zeta) = \int_{\Omega^A} \frac{1}{2}\varepsilon^A{:}\mathrm{C}^A{:}\varepsilon^A \mathrm{d}\Omega + \int_{\Omega^B} \frac{1}{2}\varepsilon^B{:}\mathrm{C}^B{:}\varepsilon^B \mathrm{d}\Omega \\ + \int_{\Gamma_c} \frac{1}{2}\Big[\zeta(k_{n_1}+\zeta k_{n_2})[\mathbf{u}]_n^2 + \zeta(k_{s_1}+\zeta k_{s_2})[\mathbf{u}]_s^2 + k_g([\mathbf{u}]_n^-)^2\Big]\mathrm{d}\Gamma, \end{aligned} \tag{3}$$

with the admissible displacements $\mathbf{u}^\eta = \mathbf{w}^\eta(\tau)$ on Γ_u^η and the small strain tensor $\varepsilon^\eta{=}\varepsilon(\mathbf{u}^\eta)$, the potential energy of external forces (acting only along the boundary in the present work):

$$\mathcal{F}(\tau,\mathbf{u}) = -\int_{\Gamma_t^A} \mathbf{f}^A{\cdot}\mathbf{u}^A \mathrm{d}\Gamma - \int_{\Gamma_t^B} \mathbf{f}^B{\cdot}\mathbf{u}^B \mathrm{d}\Gamma, \tag{4}$$

and the dissipation potential

$$\begin{aligned} \mathcal{R}(\mathbf{u};\dot{\mathbf{u}},\dot{\zeta}) = \int_{\Gamma_c} -\mu k_g[\mathbf{u}]_n^-{\cdot}|[\dot{\mathbf{u}}]_s| + G_d|\dot{\zeta}| + \frac{1}{2}\omega|\dot{\zeta}|^2 \mathrm{d}\Gamma \\ + \tau_R \int_{\Omega^A} \frac{1}{2}\dot{\varepsilon}^A{:}\mathbf{C}^A{:}\dot{\varepsilon}^A \mathrm{d}\Omega + \tau_R \int_{\Omega^B} \frac{1}{2}\dot{\varepsilon}^B{:}\mathbf{C}^B{:}\dot{\varepsilon}^B \mathrm{d}\Omega, \end{aligned} \tag{5}$$

where $\dot{\varepsilon}^\eta{=}\varepsilon(\dot{\mathbf{u}}^\eta)$ is the strain rate.

3. The numerical solution

The numerical procedures proposed for solving the above problem consider time and spatial discretization separately, as usual, see e. g. [2, 3, 8]. The procedure is formulated in terms of the boundary data only, with the spatial discretization leading to the Symmetric Galerkin BEM (SGBEM) as described in [7].

3.1. Time discretization

The time-stepping scheme is defined by a fixed time step size τ_0 such that $\tau^k{=}k\tau_0$ for $k{=}1,\dots\frac{T}{\delta}$. The displacement rate is approximated by the finite difference $\dot{\mathbf{u}}{\approx}\frac{\mathbf{u}^k-\mathbf{u}^{k-1}}{\tau_0}$, where $\mathbf{u}^k$ denotes the solution at the discrete time τ^k. Similarly the damage rate can be approximated by $\dot{\zeta}{\approx}\frac{\zeta^k-\zeta^{k-1}}{\tau_0}$. The differentiation with respect to the displacement and damage rates can be replaced by the differentiation with respect to $\mathbf{u}$ and ζ, respectively, as well, i.e.

$$\partial_{\dot{\mathbf{u}}}\mathcal{R}(\mathbf{u};\dot{\mathbf{u}},\dot{\zeta}) \approx \tau_0\partial_{\mathbf{u}}\mathcal{R}(\mathbf{u}^{k-1};\frac{\mathbf{u}-\mathbf{u}^{k-1}}{\tau_0},\frac{\zeta-\zeta^{k-1}}{\tau_0}), \tag{6}$$

$$\partial_{\dot{\zeta}}\mathcal{R}(\mathbf{u};\dot{\mathbf{u}},\dot{\zeta}) \approx \tau_0\partial_{\zeta}\mathcal{R}(\mathbf{u}^{k-1};\frac{\mathbf{u}-\mathbf{u}^{k-1}}{\tau_0},\frac{\zeta-\zeta^{k-1}}{\tau_0}). \tag{7}$$

It means that the inclusion is approximated at discrete times τ^k by the first order optimality condition for the functional

$$\mathcal{H}^k(\mathbf{u},\zeta) = \mathcal{E}(k\tau_0,\mathbf{u},\zeta) + \tau_0\mathcal{R}(\mathbf{u}^{k-1};\frac{\mathbf{u}-\mathbf{u}^{k-1}}{\tau_0},\frac{\zeta-\zeta^{k-1}}{\tau_0}) + \mathcal{F}(k\tau,\mathbf{u}). \tag{8}$$

The optimality solution is denoted by $\mathbf{u}^k$. Substituting the previous time-step result into the dissipation potential due to friction makes the pertinent functional convex with respect to the unknown $\mathbf{u}$, the optimality solution being thus unique and defining the minimum. The simple viscosity model is chosen in order to exploit the reformulation of the visco-elastic problem in the bulk in terms of an elastic problem in the bulk, which is solved by the elastostatic SGBEM [2]. Let us introduce a new variable $\mathbf{v}$ (a fictitious displacement), which will replace the admissible $\mathbf{u}$ for the time step k, as

$$\mathbf{v} = \mathbf{u} + \tau_R\frac{\mathbf{u}-\mathbf{u}^{k-1}}{\tau_0}, \quad \text{and also} \quad \mathbf{v}^k = \mathbf{u}^k + \tau_R\frac{\mathbf{u}^k-\mathbf{u}^{k-1}}{\tau_0}. \tag{9}$$

Then, the functional $\mathcal{H}^k$ is defined as

$$\begin{aligned}\mathcal{H}^k(\mathbf{v},\zeta) = \frac{\tau_0}{\tau_0{+}\tau_R}\Bigg[&\frac{1}{2}\int_{\Omega^A}\varepsilon(\mathbf{v}^A){:}\mathrm{C}^A{:}\varepsilon(\mathbf{v}^A)\mathrm{d}\Omega + \frac{1}{2}\int_{\Omega^B}\varepsilon(\mathbf{v}^B){:}\mathrm{C}^B{:}\varepsilon(\mathbf{v}^B)\mathrm{d}\Omega\\
&+\frac{1}{2}\frac{\tau_0}{\tau_0{+}\tau_R}\int_{\Gamma_c}\zeta(k_{n_1}{+}\zeta k_{n_2})\left[\mathbf{v}{+}\frac{\tau_R}{\tau_0}\mathbf{u}^{k-1}\right]_n^2 + \zeta(k_{s_1}{+}\zeta k_{s_2})\left[\mathbf{v}{+}\frac{\tau_R}{\tau_0}\mathbf{u}^{k-1}\right]_s^2 + k_g\left(\left[\mathbf{v}{+}\frac{\tau_R}{\tau_0}\mathbf{u}^{k-1}\right]_n^-\right)^2\mathrm{d}\Gamma\Bigg]\\
&+\int_{\Gamma_c}-\frac{\tau_0\mu k_g}{\tau_0{+}\tau_R}[\mathbf{u}^{k-1}]_n^-\left|[\mathbf{v}{-}\mathbf{u}^{k-1}]_s\right| - G_d\left(\zeta-\zeta^{k-1}\right) + \frac{\omega}{2\tau_0}\left(\zeta-\zeta^{k-1}\right)^2\mathrm{d}\Gamma\\
&+\frac{1}{2}\frac{\tau_R}{\tau_0}\int_{\Omega^A}\varepsilon(\mathbf{u}^{Ak-1}){:}\mathrm{C}^A{:}\varepsilon(\mathbf{u}^{Ak-1})\mathrm{d}\Omega + \frac{1}{2}\frac{\tau_R}{\tau_0}\int_{\Omega^B}\varepsilon(\mathbf{u}^{Bk-1}){:}\mathrm{C}^B{:}\varepsilon(\mathbf{u}^{Bk-1})\mathbf{d}\Omega\\
&-\int_{\Gamma_t^A}\mathbf{f}^A\cdot\left(\mathbf{v}^A+\frac{\tau_R}{\tau_0}\mathbf{u}^{Ak-1}\right)\mathrm{d}\Gamma - \int_{\Gamma_t^B}\mathbf{f}^B\cdot\left(\mathbf{v}^B+\frac{\tau_R}{\tau_0}\mathbf{u}^{Bk-1}\right)\mathrm{d}\Gamma,\end{aligned} \tag{10}$$

for any admissible $\mathbf{v}$, satisfying the condition

$$\mathbf{v}^\eta = \mathbf{w}^\eta(k\tau) + \frac{\tau_R}{\tau_0}(\mathbf{w}^\eta(k\tau)-\mathbf{w}^\eta((k-1)\tau)) = \tilde{\mathbf{w}}^\eta(k\tau)\ \text{on}\ \Gamma_u^\eta\ \text{and}\ 0\le\zeta\le\zeta^{k-1}\ \text{on}\ \Gamma_c. \tag{11}$$

It is worth observing that the viscosity in (10) is eliminated in the sense that the only energy term in the bulk associated to the unknown $\mathbf{v}$ is the elastic strain energy, $\mathbf{u}^{k-1}$ is known from the previous time step.

3.2. Spatial discretization and SGBEM

The role of the SGBEM in the present computational procedure is to provide a complete boundary-value solution from the given boundary data for each domain in order to calculate the elastic strain energy in these domains. Thus, the SGBEM code calculates unknown tractions along $\Gamma_c \cup \Gamma_u$, assuming the displacements jump at Γ_c to be known from the used minimization procedure, in the same way as proposed and tested in [6, 7].

3.3. Minimization algorithm

Once, all the boundary data (displacements and tractions) are obtained from the solution of the SGBEM code, the energy of the state given by $\mathcal{H}^k$ in (10) can be calculated. It is worth to see how it is carried out in the present implementation. The absolute value term and the term with $[\cdot]^-$ in $\mathcal{H}^k$ are replaced by new variables α and β and appropriately discretized as in [6]. Then, the discretized energy $\mathcal{H}^k$, from equation (10) can express as

$$\begin{aligned}
\frac{\tau_0+\tau_R}{\tau_0}\mathcal{H}^k(\mathbf{v},\alpha,\beta,\zeta) = {} & \int_{\Gamma^A}\frac{1}{2}\sum_p \mathbf{N}^A_{\psi p}(x)\mathbf{v}^A_p \cdot \sum_l \mathbf{N}^A_{\varphi l}(x)\mathbf{t}^A_l \mathrm{d}\Gamma + \int_{\Gamma^B}\frac{1}{2}\sum_q \mathbf{N}^B_{\psi q}(x)\mathbf{v}^B_q \cdot \sum_r \mathbf{N}^B_{\varphi r}(x)\mathbf{t}^B_r \mathrm{d}\Gamma \\
& + \int_{\Gamma_c}\left[\frac{1}{2}\left(\left(\sum_m N_{\zeta m}(x)\zeta_m\right)k_{n1} + \left(\sum_n N_{\zeta n}(x)\zeta_n\right)^2 k_{n2}\right)\left(\sum_q N^B_{\psi s q}(x)u^B_{s q} - \sum_p N^A_{\psi s p}(x)u^A_{s p}\right)^2\right. \\
& \quad + \frac{1}{2}\left(\left(\sum_m N_{\zeta m}(x)\zeta_m\right)k_{s1} + \left(\sum_n N_{\zeta n}(x)\zeta_n\right)^2 k_{s2}\right)\left(\sum_q N^B_{\psi s q}(x)u^B_{s q} - \sum_p N^A_{\psi s p}(x)u^A_{s p}\right)^2 \\
& \quad \left. + \frac{1}{2}k_g\left(\sum_q N^B_{\psi q}(x)\beta_q\right)^2 + \mu k_g\left(\sum_q N_{\psi q}(x)\beta^{k-1}_q\right)\left(\sum_q N_{\psi q}(x)\alpha_q\right)\right]\mathrm{d}\Gamma \\
& + \int_{\Gamma_c} -G_d\left(\sum_n N_{\zeta n}(x)(\zeta_n - \zeta^{k-1}_n)\right) + \frac{\omega}{2\,\tau_0}\left(\sum_n N_{\zeta n}(x)(\zeta_n - \zeta^{k-1}_n)\right)^2 \mathrm{d}\Gamma \\
& - \int_{\Gamma^A_t}\sum_p \mathbf{N}^A_{\psi p}(x)\mathbf{v}^A_p \cdot \sum_l \mathbf{N}^A_{\varphi l}(x)\mathbf{f}^A_l \mathrm{d}\Gamma - \int_{\Gamma^B_t}\sum_q \mathbf{N}^B_{\psi q}(x)\mathbf{v}^B_q \cdot \sum_r \mathbf{N}^B_{\varphi r}(x)\mathbf{f}^B_r \mathrm{d}\Gamma \\
& + \mathcal{V}(\mathbf{u}^{A\,k-1}, \mathbf{u}^{B\,k-1}, \mathbf{f}^{A\,k}, \mathbf{f}^{B\,k}), \quad (12)
\end{aligned}$$

where N^{AB}_{pq}=$N^B_{\psi q}(x^A_p)$. The functional $\mathcal{V}$ includes the data which are constant with respect to $\mathbf{v}$.

4. Numerical example

The crack onset and growth at the fibre-matrix interface has been tested numerically by a computer code, which was implemented in MATLAB. The developed numerical algorithm exploits the variationally based SGBEM to calculate the elastic solution at the interface and in each subdomain. An example presents the response of the cohesive contact model with friction in combination with small amount of viscosity. The geometry in the present study includes five infinitely long cylindrical fibre inclusions η=1, . . . , 5 with circular section of radius r=20μm embedded inside an infinite matrix, see Figure 3 (left). In the numerical calculation, the unbounded domain is replaced by a very large square fixed along its bottom face to a rigid foundation. For the case of the transversal loading, the solved example assumes the tension applied on the top part

of matrix boundary as can be clear from the Figure 3 (right). The loading process defines the prescribed displacements (*hard-device loading*) w_1 which are increasing during of the loading process. The incrementally prescribed loading is given by the relation $w_1^k = v\tau^k$, $k=1, 2, \ldots 100$ with $v=1\mu$m s^{-1} and $\tau^k = k\tau_0$, $\tau_0 = 2\times10^{-5}$s. The first-increment of the vertical displacement w_1 is further multiplied by a *load step factor*, changing from the initial value $k=1$ until the total damage of the interface becomes. In total, there where considered $k = 100$ load steps during the whole loading process.

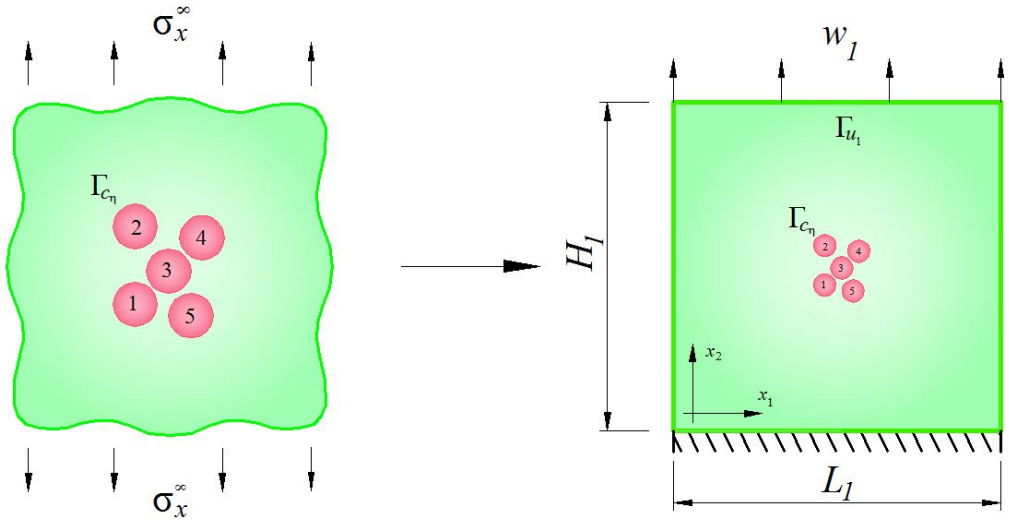

Figure 3. Replacement of the unbounded domain by a very large square matrix subjected to transversal loading.

4.1. Model properties and parameter statement

The numerical model assumes a bimaterial study that consists of epoxy matrix (m) and glass fibre (f). The dimensions of the epoxy matrix are $H_1 = 1000$ mm, $L_1 = 1000$ mm. The elastic properties of matrix and fibre are Young modules $E_m = 2\times10^3$MPa, $E_f = 20\times10^3$MPa and Poisson's ratios $\nu_m = 0.33$, $\nu_f = 0.22$. The corresponding stiffness parameters were suggested according to the cohesive contact model: the interface stiffness is defined by k_n and k_s: $k_n = 10\times10^4$MPaμm^{-1}, $k_s = 2.5\times10^4$MPaμm^{-1}. In order to obtain continuous non-linear response of the investigated variables, both normal and tangential stiffnesses were split into two parts according to the relations: $k_n = k_{n_1} + k_{n_2}$, $k_s = k_{s_1} + k_{s_2}$, $k_{n_1} = 0.01 \times k_n$, $k_{n_2} = 0.99 \times k_{n_1}$, $k_{s_1} = 0.01 \times k_s$, $k_{s_2} = 0.99 \times k_{s_1}$. The parameters that govern the crack growth are: the fracture energy $G_d = 2\times10^{-3}$Jμm^{-2} and the viscosity parameter $\omega = 1\times10^{-3}$MPa.s.

4.2. Result of the analysis of the model

The obtained numerical solution of investigated contact model is presented in following figures. The main feature occurring in the graphs is the continuous non-linear response of the mechanical stress t and damage parameter ζ, see Figures 4, 5. The Figure 4 presents the evolution of damage parameter ζ at interface of the inclusion $\eta=4$ at load steps $k=12, 13, 14, 15$. The influence of cohesive continuous dependence is obvious, after the system reaches the required amount of fracture energy G_d. In agreement with aforementioned cohesive-contact theory [3], let us mention that the evolution of damage parameter ζ changes from one to zero continuously and thus preserves the continuous character of the debonding process. Figure 6 presents the de-

formed shapes of the debonding problem for 3 different loadsteps, respectively. It is noteworthy that achieved results of deformations reflect the progress in crack propagation at fibre-matrix interface analogously as in the study of Távara et. al. [4, 5]

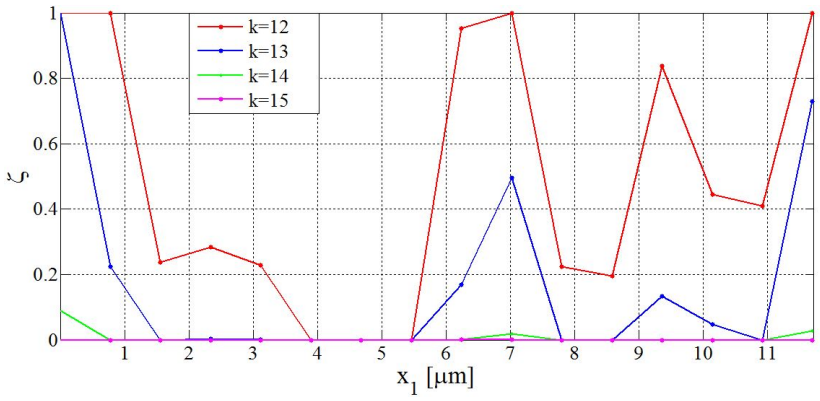

Figure 4. Distributiion of damage parameter ζ for the fibre η=4 at particular loadsteps.

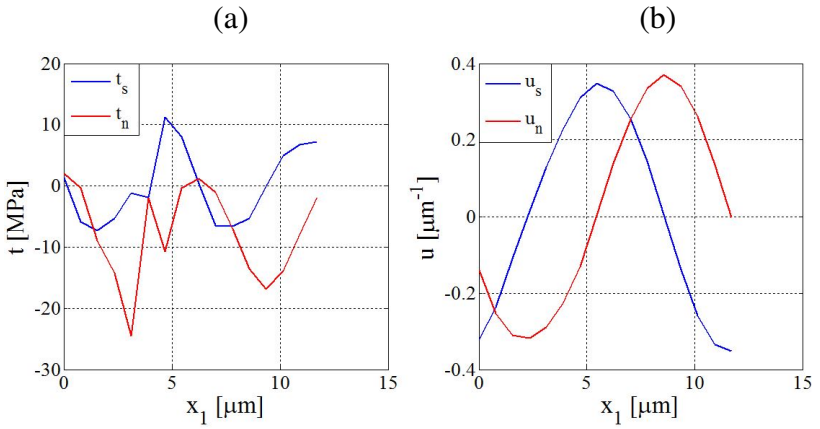

Figure 5. Distribution of (a) stress t, (b) displacement u for the fibre η=4 at loadsteps12.

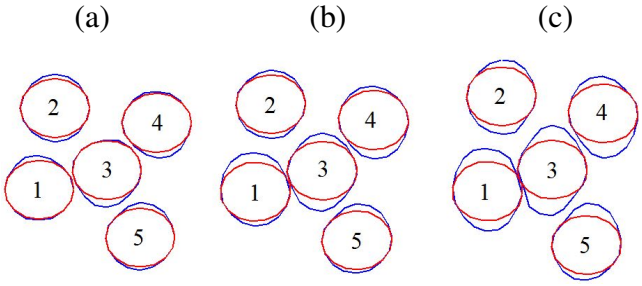

Figure 6. Deformed shape of at the scale of fibres corresponding to loadsteps (a) k=13, (b) k=15, (c)=25.

5. Conclusions

An energy based model for study a fibre-matrix debonding problem is presented. The proposed numerical model provides an approach which combines the cohesive contact at the fibre-matrix interface with at least a small amount of viscosity to make the solution more regular for mathematical treatment. Especially, this model has been used to characterize the crack onset and growth in a fibre bundle embedded in an infinite matrix subjected to transverse loading. The

numerical implementation of spatial discretization *via* SGBEM has permitted the whole problem to be defined only by a boundary and interface data. The obtained results document the evolution of the debonding at the fibre-matrix interface during the whole loading process. The cohesiveness of the contact is stressed by new energy terms depending non-linearly on the damage parameter ζ together with pertinent stiffness parameters providing required non-linear continuous response in investigated quantities. The present results confirm the expected behaviour in accordance with previous studies of fibre-matrix debonding and asses its applicability in the area of composite materials.

6. Acknowledgement

The authors acknowledge the financial support from the Grant Agency of Slovak Republic. The project number is VEGA 1/0201/11. The work was also supported by Slovak Academic Information Agency through the National Scholarship Programme of the Slovak Republic.

References

[1] Dostál, Z. *Optimal Quadratic Programming Algorithms*, *Springer Optimization and Its Applications.* Springer, Berlin, volume 23, 2009.

[2] Roubíček, T., Panagiotopoulos, C.G. and Mantič, V. Quasistatic adhesive contact of viscoelastic bodies and its numerical treatment for very small viscosity. *ZAMM – Zeitschrift Angew. Math. Mech.* volume 93, 2013.

[3] Roubíček, T., Kružík, M. and Zeman, J. Delamination and adhesive contact models and their mathematical analysis and numerical treatment (Chapter 9). In V. Mantič, editor, *Mathematical Methods and Models in Composites*, Imperial College Press, 2013.

[4] Távara, L., Mantič, V., Graciani, E. and París, F. BEM analysis of crack onset and propagation along fiber-matrix interface under transverse tension using a linear elastic-brittle interface model. *Engineering Analysis with Boundary Elements.* volume 35:207–222, 2011.

[5] Távara, L., Mantič, V., Graciani, E. and París, F. BEM modelling of interface cracks in a group of fibres under biaxial transverse loads. *Advances in Boundary Element and Meshless Techniques XIV*, Eastleigh : EC ltd., volume 14, Paris, 2013.

[6] Vodička, R. and Mantič, V. An SGBEM implementation with quadratic programming for solving contact problems with Coulomb friction. *Advances in Boundary Element and Meshless Techniques XIV*, Eastleigh : EC ltd., volume 14, Paris, 2013.

[7] Vodička, R., Mantič, V. and París, F. Symmetric variational formulation of BIE for domain decomposition problems in elasticity - an SGBEM approach for nonconforming discretizations of curved interfaces. *Comp. Model. Eng.*,volume 17, pages 173–203, 2007.

[8] Vodička, R., Mantič, V. and Roubíček, T. An SGBEM implementation of quasi–static rate–independent mixed-mode delamination model. Submitted to *Meccanica*, 2014.